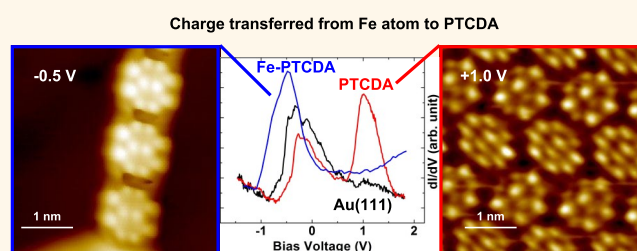


Digitized Charge Transfer Magnitude Determined by Metal–Organic Coordination Number

Hung-Hsiang Yang,[†] Yu-Hsun Chu,[†] Chun-I Lu,[†] Tsung-Han Yang,[†] Kai-Jheng Yang,[†] Chao-Cheng Kaun,[‡] Germar Hoffmann,[†] and Minn-Tsong Lin^{†,§,*}

[†]Department of Physics, National Taiwan University, Taipei, Taiwan and [‡]Research Center for Applied Sciences and [§]Institute of Atomic and Molecular Sciences, Academia Sinica, Taipei, Taiwan

ABSTRACT Well-ordered metal–organic nanostructures of Fe-PTCDA (perylene-3,4,9,10-tetracarboxylic-3,4,9,10-dianhydride) chains and networks are grown on a Au(111) surface. These structures are investigated by high-resolution scanning tunneling microscopy. Digitized frontier orbital shifts are followed in scanning tunneling spectroscopy. By comparing the frontier energies with the molecular coordination environments, we conclude that the specific coordination affects the magnitude of charge transfer onto each PTCDA in the Fe-PTCDA hybridization system. A basic model is derived, which captures the essential underlying physics and correlates the observed energetic shift of the frontier orbital with the charge transfer.



KEYWORDS: scanning tunneling microscopy · scanning tunneling spectroscopy · metal–organic coordination · self-assembled nanostructure · charge transfer

Electron transport through metal–organic heterostructures in organic electronics strongly depends on the interface formed between the metal atom and the organic molecule in terms of geometry and electronic configuration.¹ In particular, the charge redistribution within the metal–organic interface plays a crucial role for electrical, optical, and magnetic properties which are relevant in technological applications such as organic light-emitting diodes, field-effect transistors,^{2,3} organic solar cells,^{4,5} and organic spin valves.⁶ To improve the performance of organic devices requires more detailed understanding of the local mechanisms responsible for the charge transfer between metals (small ionization potential) and molecules (larger electron affinity with respect to metals). Metal–organic complexes have attracted widespread interest in the past decade,⁷ particularly for their electronic and magnetic properties.^{8,9} The growth of predefined metal–organic structures has been achieved by the appropriate choice of head groups and molecular ligands.^{10,11} Thus, various coordination geometries can be engineered in

such metal–organic structures,¹² which provide different chemical environments for molecules. A nonlocal approach measurement (X-ray photoemission spectroscopy) combined with preliminary scanning tunneling microscopy (STM) topography shows various oxidation states of both metal atoms and organic molecules in coordination networks.¹³

PTCDA (chemical structure in Figure 1a) is a large π -conjugated organic molecule, which has been used in the fabrication of organic thin-film transistors,¹⁴ organic light-emitting diodes,¹⁵ and organic spin valves.¹⁶ Self-assembled structures on various substrates such as Ag(111) and Au(111) are reported.^{17–22} Molecules remain nondistorted on Au(111) which refers to a physisorption. Weak interaction between PTCDA and Au(111) substrate results in high molecular mobility even at reduced temperatures. Therefore, Au(111) is a suitable substrate for PTCDA to form metal–organic complexes. In a recent work,²³ the appearance of self-assembled PTCDA in contact with a metallic substrate [Au(111)] was investigated by STM. Furthermore,

* Address correspondence to mtlin@phys.ntu.edu.tw.

Received for review January 23, 2013 and accepted March 1, 2013.

Published online March 01, 2013
10.1021/nn4003715

© 2013 American Chemical Society

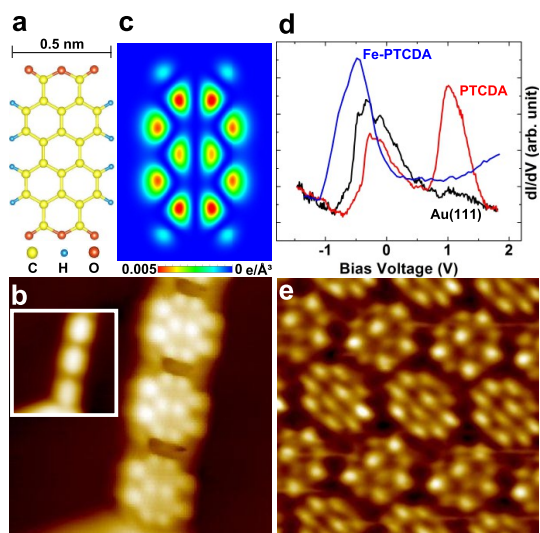


Figure 1. (a) PTCDA chemical structure. (b) STM image ($4 \times 4 \text{ nm}^2$) of Fe-PTCDA chain structure with the frontier orbital resolved at -0.5 V (inset: $4 \times 4 \text{ nm}^2$, $+1.8 \text{ V}$). (c) PTCDA projected frontier orbital. (d) Spectroscopy recorded on gold surface (black curve), for self-assembled PTCDA (red curve) and PTCDA in an Fe-PTCDA chain structure (blue curve). (e) STM image ($4 \times 4 \text{ nm}^2$) of self-assembled PTCDA with the frontier orbital visible at $+1.0 \text{ V}$. (The main reason for the asymmetry of the appearance of PTCDA in a different row might be due to the asymmetry of the tip state.)

Méndez *et al.* made an interesting observation when they additionally introduced Fe adsorbates. Metal–organic networks, such as Fe-PTCDA chains²⁴ and two-dimensional structures,²⁵ were controllably formed. These room-temperature STM experiments revealed a modification of the electronic structure. Accompanying density functional theory (DFT) calculations suggested a charge transfer between Fe atoms and PTCDA.²⁵ To gain deeper insight into how the molecular electronic structure is modified by the formation of a molecule–metal interface and the peculiar role of the Fe, precise and laterally resolved spectroscopy data are required. In this article, first low-temperature STM and scanning tunneling spectroscopy (STS) results are presented, which reveal the effect of the local environment on the charge state on a single-molecule scale. We find digitized charge states of PTCDA which are determined by the coordination number of Fe atoms and neighboring molecules in self-assembled networks.

RESULTS AND DISCUSSION

Figure 1b shows a representative STM image of an Fe-PTCDA chain structure as acquired at -0.5 V . The intramolecular structure of PTCDA in the chain shows mirror symmetry along both the short and long axis of the molecule, revealing two lobes for the outer and three for the inner part. This orbital structure has been identified as the lowest unoccupied molecular orbital (LUMO) of gas phase PTCDA in DFT calculations (Figure 1c). In the following, the LUMO is called frontier orbital (frontier orbital is defined as the state which is

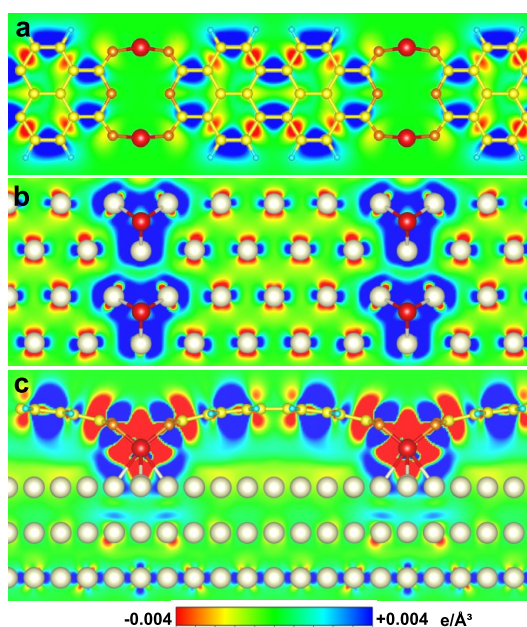


Figure 2. Charge transfer map in different cross sections with colors indicating the amount of transferred charges in comparison to the neutral region (green). Red indicates a reduction of electron density and blue an enhancement. (a) In the molecular plane, molecules accept electrons with the amount modulated over the entire molecule. (b) In the Au layer underneath, in the vicinity of the Fe atoms, electrons are accumulated in the Au layer. (c) Perpendicular cross section, Fe donates electrons to its environment.

the nearest to the Fermi level and relevant for chemical reactivity²⁶) while discussing the LUMO shifting from positive to negative energy. Molecules in the inset of Figure 1b show no obvious internal structure at $+1.8 \text{ V}$. This suggests an occupied state for molecules in the chain. Figure 1d presents STS results of Fe-PTCDA (blue curve), PTCDA (red curve), and Au(111) surface (black curve). The spectroscopy curve on Fe-PTCDA shows a peak at around -0.4 V which originates from the frontier orbital. For self-assembled PTCDA, the STS data reveal two peaks at $+1 \text{ V}$ and -0.4 V . The former one is the frontier orbital state of self-assembled PTCDA. The latter one is the surface state mediated by the first PTCDA film at reduced intensity and shifted peak position.²³ Respectively, the frontier orbital is imaged as an unoccupied state in STM (see Figure 1e). After the formation of Fe-PTCDA chains, the formerly unoccupied frontier orbital of the PTCDA dominates the appearance of PTCDA within the chains for negative bias (Figure 1b); that is, the frontier orbital is now an occupied state. This detail was not resolved in previous room-temperature experiments.

To investigate the charge transfer behavior, DFT calculations have been performed for the Fe-PTCDA chain structure adsorbed on a Au(111) surface. In Figure 2a, we verified that the chain structure with two bridging Fe atoms is the energetic minimum geometry (see Methods section). According to the relaxed geometry of the chain structure, Fe atoms

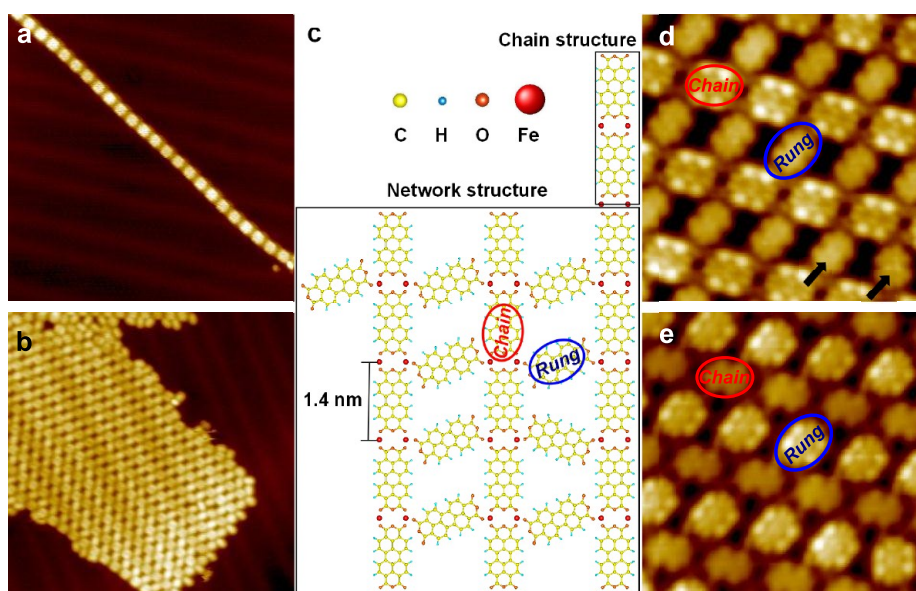


Figure 3. STM image of Fe-PTCDA (a) chain and (b) network structure (each $30 \times 30 \text{ nm}^2$, -1.0 V) along with a (c) schematic representation. STM images ($5.7 \times 5.7 \text{ nm}^2$) of the same network structure as recorded at (d) -0.5 V and (e) $+0.5 \text{ V}$. Thereby, the frontier orbital is an occupied state for chain-PTCDA and an unoccupied state for rung-PTCDA. The arrows in (d) indicate two rung-PTCDAs which are rotated against each other.

adsorb on top of the hollow Au(111) site (see Figure 2b). PTCDA molecules, which coordinate with Fe atoms, are bent and lifted (Figure 2c). As a consequence, Fe atoms are below the plane of the molecules. Figure 2 shows the charge accumulation (blue) and depletion (red) of the hybridized chain structures on Au(111) surface on three planes: the molecular plane (Figure 2a), the Au surface (Figure 2b), and the orthogonal plane contains the Fe atoms (Figure 2c). The results show that the Fe atoms donate electrons to both molecules and the Au(111) surface. Each Fe atom (there are two in every unit cell) gives 0.97 electrons to its adjacent environment, where each molecule accepts 1.11 electrons and the gold surface accepts 0.83 electrons per unit cell. Combining STS spectroscopy and the appearance of the orbital structure obtained by STM, we can identify the energy shift of the molecular state due to the charging effect of molecules. Furthermore, the DFT results show that the environment of Fe atoms, including neighboring molecules and Au atoms, is relevant for the charge redistribution.

Depending on the preparation conditions, chain structures (Figure 3a) and network structures (Figure 3b) are created (see the Methods section). Following Méndez *et al.*,²⁴ chain structures are stabilized by two iron atoms connecting with dianhydride groups from two PTCDA molecules, while networks are constructed by several chains interconnected by PTCDA molecules. In the work of Alvarez *et al.*,²⁵ a perpendicular arrangement of interconnecting PTCDA molecules is suggested. From our high-resolution data, a modified structure with rotated PTCDA molecules can be deduced (Figure 3c). Although a preferentially parallel alignment of interconnecting PTCDA molecules is observed within ordered structures, at a low frequency,

oppositely rotated PTCDA molecules are identified (see Figure 3d, arrows). For convenience, PTCDA connected to four Fe atoms is called chain-PTCDA and interconnecting PTCDA is called rung-PTCDA. A significant variation of the electronic structure is indicated by the energy at which the frontier orbital is resolved in STM. From STM images (Figure 3d,e), we find a strong bias-dependent appearance of molecules. In chain-PTCDA, the STM image at -0.5 V (Figure 3d) shows the frontier orbital appearance, which appears at $+0.5 \text{ V}$ in Figure 3e. Considering that the binding mechanism is different for the two PTCDA species between the occupied and unoccupied frontier orbitals, we expect that an environment-dependent charge transfer occurs.

Figure 4a demonstrates spectra of molecules in different environments. For all spectra, we find a peak at the energy of the Au(111) surface state. In addition, unoccupied molecular states are identified. Thereby, the energetically lowest state (*i.e.*, the frontier orbital) is easily identified in STM data by its characteristic appearance. As a consequence, the spectra in Figure 4a are sorted by the energy of the frontier orbital. In Figure 4b, the respective positions of acquisition are indicated. Molecules with different energies are respectively labeled A, B, C, and D.

A direct correlation between the energetic shift and the environment is striking. The frontier orbital of the molecule at the edge (A) attached to only one Fe has the highest energy (1.23 eV). Molecules denoted by B, B', and B'' give the identical electronic signature. These molecules have two Fe atoms attached but different binding orientations. Thereby, whether the molecule is attached at both ends each to one Fe (B) or at one end to two Fe atoms (B', B'') does not influence the charge

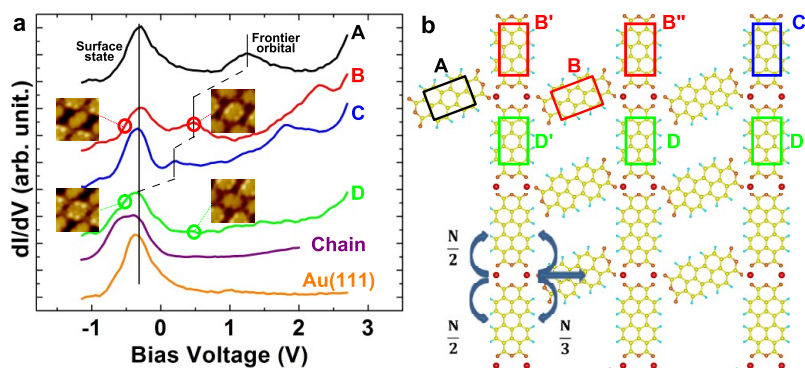


Figure 4. (a) STS curves on molecules in different bonding environments. The frontier orbital shifts to lower energies upon coordination with Fe. Once occupied, the frontier orbital is pinned by the surface state of Au(111), which is mediated through the molecular layer at lower coordination (Note: variation of the detailed line shapes has to be attributed to the usage of different tips; see Supporting Information). Inset: STM images show the appearances of B and D molecules at indicated (red and green circles) bias voltages. (b) Indicates the originating positions. Thereby, labels A–D indicate all characteristic structures. An electron donation (blue arrows) from the Fe to neighboring PTCDA is deduced with the amount of charge accepted by each PTCDA depending on the local geometry ($N/2$ or $N/3$, where $N = 0.56$).

transfer. However, the environment of the attached Fe atom is relevant. The molecule labeled by C also has two neighboring Fe atoms but differs in energy from molecule B; one Fe connects to three, while the other one only contacts two PTCDA. Interesting is also the case of the molecule denoted by D (as well as within chains). Spectra from these molecules show no additional peak apart from the surface state of the underlying Au(111) substrate. However, STM imaging gives evidence that a molecular state is present. This is demonstrated in the insets of Figure 4a. We therefore conclude that the frontier orbital hybridizes with the Au(111) surface state and is pinned at its energy. For molecules A, B, and C, the frontier orbital is unoccupied and recorded in STM at positive bias, whereas for molecule D, the frontier orbital is occupied and the characteristic appearance is not observed at positive but at negative bias.

The shift of the frontier orbital from an unoccupied to occupied state gives direct evidence for a charge transfer process. We interpret the energetic shift for A, B, and C as the consequence of a charge transfer and a respective distribution over the neighboring molecules which is correlated to the coordination. It is instructive to first revisit recently obtained results on artificially created metal–organic junctions. Repp *et al.*²⁷ achieved a charging of pentacene molecules by attaching Au atoms by STM manipulation. Electronically decoupled from the substrate through an insulating layer, the acceptance of one (or more) electron causes the occupation of one (or more) previously unoccupied state. Yamachika *et al.*²⁸ observed a linear shifting of the LUMO+1 of C_{60} by controlling the amount of attaching K atoms. The linear shifting originates from the charge transfer from K to the LUMO of C_{60} , resulting from a constant number of electrons provided by each K atom. Different to Repp *et al.*, we do not observe for A–C the crossing of the Fermi level

(Figure 4a). Instead, we observe only an energetic shift. To explain our observation, we estimate that every Fe atom donates 0.56 electrons to the molecule. These donor electrons are equally distributed among the neighboring PTCDA. Therefore, each Fe atom gives $0.56/n$ electrons to PTCDA, where n is the number of the neighboring molecules. The isotropic distribution of electrons can be deduced from the comparison of B versus B', the relevance of the number of attached PTCDA from the comparison of molecules B'' and C. This heuristically developed picture is applied to the structure presented in Figure 4b. In Figure 4b, we find that, within a self-assembled network, PTCDAs are attached to one (at the edge) up to four Fe atoms (chain-PTCDA). As a consequence, the total number of molecular accepted electrons α varies and is determined as $\alpha = \sum_i (N/n_i)$, (i = index of connected Fe atoms and $N = 0.56$).

Figure 5 presents the digitized energies of the frontier orbital for all observed coordination geometries plotted against the total number of accepted electrons α . The graph reveals a linear relation (red line, the slope is -0.34 eV/e) between the accepted electron number and the frontier orbital energy. The digitized shifts are in accordance with Yamachika *et al.*, which supports our interpretation that the observed shifts are the response to a charging event. The reason for the digitized shifts is due to electrons partially occupying the broadened molecular state which are due to the hybridization with the substrate and Fe atoms. Therefore, we observed the frontier orbital shifts while the Fermi level is filled up. However, a peculiar involvement of the substrate by the formation of molecule–substrate hybrid states is also expected. These molecule–substrate hybrid states might result in states with energy between the LUMO and the Fermi level. Moreover, the frontier orbital of the tungsten tip and the hybrid states is localized, therefore, the hybrid

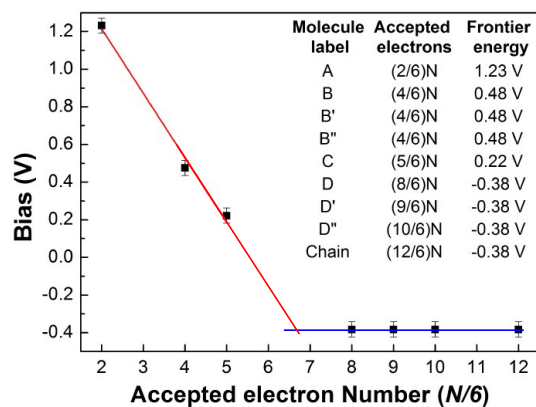


Figure 5. Accepted electron number of the molecule against the energy of its frontier orbital. A linear relation (red line, -0.34 eV/e) is identified. After accepting (8/6) N electrons, a saturation of the shift is observed and the energy of the frontier orbital remains constantly at the energy of the Au(111) surface state (blue line). All values are summarized in the inset with the molecular label referring to Figure 3.

states cannot be probed above the molecule.²⁹ Furthermore, above acceptance of (8/6) Ne^- , a saturation is observable (blue line). The number of accepted electrons for molecules in D and chains are different but reveal the identical frontier orbital peak center. To explain the saturation point, we expect a peculiar involvement of the substrate as a host of electrons. A saturation of the shifts indicates a limitation of the number of electrons which can be accepted by a PTCDA molecule. Surface states of substrates may determine such a limitation and provide an electron

reservoir. Result from this is that, once the frontier orbital is pinned by the surface state, the energy remains fixed independent of the environment and the electrons energetically prefer to go into the surface.³⁰ These results are in accordance with our DFT calculations. Electrons are also transferred into the Au(111) surface in the chain structure, which is the heavy saturated system in our analysis.

CONCLUSION

In conclusion, we studied self-assembled Fe-PTCDA networks by STM and STS supported by DFT calculations. Thereby, different metal–organic coordination and charge states of molecules are provided. We identified digitized frontier orbital energy shifts which are related to the local metal–organic coordination. In the assembled structures, the Fe atom plays the role of an electron donor. Donated electrons are equally shared among adjacent molecules. Our data indicate that the characteristic frontier orbital is preserved after the charge transfer process but shifted in energy proportional to the amount of accepted electrons. Our findings, which are related to the charge redistribution at metal–organic interfaces on the molecular scale, are important to understand the energy level alignment.³¹ As a result, the ability to design the network structure by binding metal atoms with organic molecules offers a unique way to engineer the oxidation state of involved molecules as also relevant for molecular magnetism⁸ and superconductivity.³²

METHODS

Measurements were performed in an Omicron ultrahigh vacuum low-temperature STM. Sample temperatures were maintained at 4.5 and 77.7 K during experiments with equivalent results obtained. After cycles of Ar^+ sputtering and annealing processes for Au(111) substrate preparation, PTCDA (rate: 0.01 ML/s, sublimation temperature ~ 550 K) and Fe (rate: 0.02 ML/s) were dosed onto the room-temperature sample surfaces. Upon a final annealing step to ~ 400 K, molecule–metal networks were formed. Thereby, when PTCDA was prepared after Fe deposition, a dense Fe-PTCDA network was formed; otherwise, chains structures were predominant. For scanning tunneling spectroscopy, a modulation voltage ($\Delta U = 40$ mV, $f = 5.9$ kHz) was added to the bias voltage and the induced current modulation was recorded *via* lock-in techniques. Thereby, positive (negative) bias voltages refer to tunneling into unoccupied (out-of-occupied) states. Curves on molecules were extracted from two-dimensional data sets. Every STS curve was taken at the center of a molecule and averaged over ~ 50 spectra (area ~ 0.3 nm²).

The geometry structure relaxation was performed with Quantum ESPRESSO.³³ We chose GGA pseudopotential³⁴ to get the optimized geometry relaxation. The cut off kinetic energy and charge density were 20 and 240 Ry, respectively. The Brillouin zone was sampled at the Γ reciprocal point.³⁵ For the Fe-PTCDA chain on the Au(111) system, there were 1492 electrons per unit cell. The convergence condition is that the force acting on each atom was smaller than 10^{-3} Ry/ a_0 . In order to calculate the electronic structure, we used Nanodcal³⁶ DFT package with LCAO basis. The Brillouin zone was sampled with $5 \times 10 \times 1$

reciprocal points.³⁵ The spacing between two slabs was 22.5 Å, which ensured that the system was isolated in the z-direction. We used LDA exchange correlation for electronic structure calculations.

Conflict of Interest: The authors declare no competing financial interest.

Acknowledgment. This work was supported in part by the National Science Council of Taiwan through Grant No. NSC 101-2120-M-002-012.

Supporting Information Available: Complete STS curves on molecules A–D in Figure 3 with different tips. The STS curves taken at different atomic position of molecules C and D' are included. This material is available free of charge *via* the Internet at <http://pubs.acs.org>.

REFERENCES AND NOTES

- Nazin, G. V.; Qiu, X. H.; Ho, W. Visualization and Spectroscopy of a Metal–Molecule–Metal Bridge. *Science* **2003**, *302*, 77–81.
- Moons, E. Conjugated Polymer Blends: Linking Film Morphology to Performance of Light Emitting Diodes and Photodiodes. *J. Phys.: Condens. Matter* **2002**, *14*, 12235–12260.
- Cicoira, F.; Santato, C. Organic Light Emitting Field Effect Transistors: Advances and Perspectives. *Adv. Funct. Mater.* **2007**, *17*, 3421–3434.

- Blom, P.; Mihailetchi, V.; Koster, L.; Markov, D. Device Physics of Polymer: Fullerene Bulk Heterojunction Solar Cells. *Adv. Mater.* **2007**, *19*, 1551–1566.
- Brabec, C. J.; Sariciftci, N. S.; Hummelen, J. C. Plastic Solar Cells. *Adv. Funct. Mater.* **2001**, *11*, 15–26.
- Barraud, C.; Seneor, P.; Mattana, R.; Fusil, S.; Bouzehouane, K.; Deranlot, C.; Graziosi, P.; Hueso, L.; Bergenti, I.; Dediu, V.; *et al.* Unravelling the Role of the Interface for Spin Injection into Organic Semiconductors. *Nat. Phys.* **2010**, *6*, 615–620.
- Barth, J. V. Molecular Architectonic on Metal Surfaces. *Annu. Rev. Phys. Chem.* **2007**, *58*, 375–407.
- Abdurakhmanova, N.; Floris, A.; Tseng, T.-C.; Comisso, A.; Stepanow, S.; De Vita, A.; Kern, K. Stereoselectivity and Electrostatics in Charge-Transfer Mn- and Cs-TCNQ₄ Networks on Ag(100). *Nat. Commun.* **2012**, *3*, 940.
- Gambardella, P.; Stepanow, S.; Dmitriev, A.; Honolka, J.; de Groot, F. M. F.; Lingenfelder, M.; Gupta, S. S.; Sarma, D. D.; Bencok, P.; Stanescu, S.; *et al.* Supramolecular Control of the Magnetic Anisotropy in Two-Dimensional High-Spin Fe Arrays at a Metal Interface. *Nat. Mater.* **2009**, *8*, 189–193.
- Stepanow, S.; Lin, N.; Payer, D.; Schlickum, U.; Klappenberger, F.; Zoppellaro, G.; Ruben, M.; Brune, H.; Barth, J. V.; Kern, K. Surface-Assisted Assembly of 2D Metal-Organic Networks That Exhibit Unusual Threefold Coordination Symmetry. *Angew. Chem., Int. Ed.* **2007**, *46*, 710–713.
- Klyatskaya, S.; Klappenberger, F.; Schlickum, U.; Kühne, D.; Marschall, M.; Reichert, J.; Decker, R.; Krenner, W.; Zoppellaro, G.; Brune, H.; *et al.* Surface-Confined Self-Assembly of Di-carbonitrile Polyphenyls. *Adv. Funct. Mater.* **2011**, *21*, 1230–1240.
- Schlickum, U.; Klappenberger, F.; Decker, R.; Zoppellaro, G.; Klyatskaya, S.; Ruben, M.; Kern, K.; Brune, H.; Barth, J. V. Surface-Confined Metal-Organic Nanostructures from Co-directed Assembly of Linear Terphenyl-dicarbonitrile Linkers on Ag(111). *J. Phys. Chem. C* **2010**, *114*, 15602–15606.
- Li, Y.; Xiao, J.; Shubina, T. E.; Chen, M.; Shi, Z.; Schmid, M.; Steinrück, H.-P.; Gottfried, J. M.; Lin, N. Coordination and Metalation Bifunctionality of Cu with 5,10,15,20-Tetra-(4-pyridyl)porphyrin: Toward a Mixed-Valence Two-Dimensional Coordination Network. *J. Am. Chem. Soc.* **2012**, *134*, 6401–6408.
- Ostrick, J. R.; Dodabalapur, A.; Torsi, L.; Lovinger, A. J.; Kwock, E. W.; Miller, T. M.; Galvin, M.; Berggren, M.; Katz, H. E. Conductivity-Type Anisotropy in Molecular Solids. *J. Appl. Phys.* **1997**, *81*, 6804–6808.
- Shen, Z.; Burrows, P. E.; Bulović, V.; Forrest, S. R.; Thompson, M. E. Three-Color, Tunable, Organic Light-Emitting Devices. *Science* **1997**, *276*, 2009–2011.
- Li, K.-S.; Chang, Y.-M.; Agilan, S.; Hong, J.-Y.; Tai, J.-C.; Chiang, W.-C.; Fukutani, K.; Dowben, P.; Lin, M.-T. Organic Spin Valves with Inelastic Tunneling Characteristics. *Phys. Rev. B* **2011**, *83*, 172404.
- Eremtchenko, M.; Schaefer, J. A.; Tautz, F. S. Understanding and Tuning the Epitaxy of Large Aromatic Adsorbates by Molecular Design. *Nature* **2003**, *425*, 602–605.
- Chizhov, I.; Kahn, A.; Scoles, G. Initial Growth of 3,4,9,10-Perylenetetracarboxylic-dianhydride (PTCDA) on Au(111): A Scanning Tunneling Microscopy Study. *J. Cryst. Growth* **2000**, *208*, 449–458.
- Wagner, T. Growth of 3,4,9,10-Perylenetetracarboxylic-dianhydride Crystallites on Noble Metal Surfaces. *Org. Electron.* **2004**, *5*, 35–43.
- Huang, H.; Chen, S.; Gao, X.; Chen, W.; Wee, A. T. S. Structural and Electronic Properties of PTCDA Thin Films on Epitaxial Graphene. *ACS Nano* **2009**, *3*, 3431–3436.
- Hauschild, A.; Karki, K.; Cowie, B.; Rohlfing, M.; Tautz, F.; Sokolowski, M. Molecular Distortions and Chemical Bonding of a Large π -Conjugated Molecule on a Metal Surface. *Phys. Rev. Lett.* **2005**, *94*, 036106.
- Henze, S.; Bauer, O.; Lee, T.-L.; Sokolowski, M.; Tautz, F. Vertical Bonding Distances of PTCDA on Au(111) and Ag(111): Relation to the Bonding Type. *Surf. Sci.* **2007**, *601*, 1566–1573.
- Nicoara, N.; Román, E.; Gómez-Rodríguez, J. M.; Martín-Gago, J. A.; Méndez, J. Scanning Tunneling and Photoemission Spectroscopies at the PTCDA/Au(111) Interface. *Org. Electron.* **2006**, *7*, 287–294.
- Méndez, J.; Caillard, R.; Otero, G.; Nicoara, N.; Martín-Gago, J. Nanostructured Organic Material: From Molecular Chains to Organic Nanodots. *Adv. Mater.* **2006**, *18*, 2048–2052.
- Alvarez, L.; Peláez, S.; Caillard, R.; Serena, P. A.; Martín-Gago, J. A.; Méndez, J. Metal-Organic Extended 2D Structures: Fe-PTCDA on Au(111). *Nanotechnology* **2010**, *21*, 305703.
- Fukui, K. Role of Frontier Orbitals in Chemical Reactions. *Science* **1982**, *218*, 747.
- Repp, J.; Meyer, G.; Paavilainen, S.; Olsson, F. E.; Persson, M. Imaging Bond Formation between a Gold Atom and Pentacene on an Insulating Surface. *Science* **2006**, *312*, 1196–1199.
- Yamachika, R.; Grobis, M.; Wachowiak, A.; Crommie, M. F. Controlled Atomic Doping of a Single C₆₀ Molecule. *Science* **2004**, *304*, 281–284.
- Hu, Z.; Chen, L.; Zhao, A.; Li, Z.; Wang, B.; Yang, J.; Hou, J. G. Detecting a Molecule-Surface Hybrid State by an Fe-Coated Tip with a Non-s-like Orbital. *J. Phys. Chem. C* **2008**, *112*, 15603–15606.
- Vitali, L.; Levita, G.; Ohmann, R.; Comisso, A.; De Vita, A.; Kern, K. Portrait of the Potential Barrier at Metal-Organic Nanocontacts. *Nat. Mater.* **2010**, *9*, 320–323.
- Ishii, B. H.; Sugiyama, K.; Ito, E.; Seki, K. Energy Level Alignment and Interfacial Electronic Structures at Organic/Metal and Organic/Organic Interfaces. *Adv. Mater.* **1999**, *8*, 605–625.
- Clark, K.; Hassanien, A.; Khan, S.; Braun, K.-F.; Tanaka, H.; Hla, S.-W. Superconductivity in Just Four Pairs of (BETS)₂GaCl₄ Molecules. *Nat. Nanotechnol.* **2010**, *5*, 261–265.
- Giannozzi, P.; Baroni, S.; Bonini, N.; Calandra, M.; Car, R.; Cavazzoni, C.; Ceresoli, D.; Chiarotti, G. L.; Cococcioni, M.; Dal Corso, A.; *et al.* QUANTUM ESPRESSO: A Modular and Open-Source Software Project for Quantum Simulations of Materials. *J. Phys.: Condens. Matter* **2009**, *21*, 395502.
- Langreth, D. C.; Perdew, J. P. Theory of Nonuniform Electronic Systems. I. Analysis of the Gradient Approximation and a Generalization that Works. *Phys. Rev. B* **1980**, *21*, 5469–5493.
- Monkhorst, H. J.; Pack, J. D. Special Points for Brillouin-Zone Integrations. *Phys. Rev. B* **1976**, *13*, 5188–5192.
- <http://nanoacademic.ca/>.